Chem. Res. Chin. Univ., 2016, 32(5), 808—811 doi: 10.1007/s40242-016-6141-3

Effect of Structural Properties of Mesoporous Co_3O_4 Catalysts on Methane Combustion

JIA Yongchang, WANG Shuyuan, LU Jiqing and LUO Mengfei*

Key Laboratory of the Ministry of Education for Advanced Catalysis Materials, Institute of Physical Chemistry,
Zhejiang Normal University, Jinhua 321004, P. R. China

Abstract Highly ordered 2D and 3D-Co_3O_4 catalysts were prepared using SBA-15 and KIT-6 as templates. Nano-Co_3O_4 catalyst was obtained by calcination of cobalt nitrate as a comparison. The BET surface area of nano-Co_3O_4, 2D-Co_3O_4 and 3D-Co_3O_4 catalysts was 16.2, 63.9 and 75.1 m^2/g, respectively. All the catalysts were tested for the total combustion of methane and their catalytic performance was in the order of 3D-Co_3O_4(T_{90}=355 °C)> 2D-Co_3O_4(T_{90}=383 °C)>nano-Co_3O_4(T_{90}=455 °C). It was also found that the order of the areal specific reaction rates for the combustion of methane followed the same order of total activity. The characterization result demonstrates that enhanced catalytic performance of methane of the 2D-Co_3O_4 and 3D-Co_3O_4 catalysts is due to their pronounced reducibility and abundant active Co^{3+} species, which was caused by the preferential exposure of {220} crystal planes in 3D-Co_3O_4 and 2D-Co_3O_4 catalysts compared to the nano-Co_3O_4.

Keywords Mesoporous Co_3O_4; Hard template; CH_4 oxidation; KIT-6; SBA-15

1 Introduction

Noble metal catalysts are the most commonly employed systems for methane combustion, such as Au, Pd and Pt[1—4]. In spite of the excellent activity and stability, their applications have been limited by the high costs. Alternatively, transition metal oxides have attracted considerable attention in recent years, among which cobalt oxide is regarded as the most efficient catalyst in methane combustion. For example, Hu *et al.*[5] reported that the Co_3O_4 nanosheets showed better catalytic activity for CH_4 oxidation than Co_3O_4 nanobelts and nanocubes in spite of their low specific surface area. The catalytic behaviors of the catalysts for methane combustion are usually governed by the activation of methane and/or oxygen on the catalyst surface[6], which is often related to the exposed crystal planes of the catalysts. In addition, the growth of catalyst particles might be influenced by the surrounding environment, for example, the channels of the template may exert a confinement effect on the epitaxy of the catalyst and consequently the exposed planes. Garcia *et al.*[7] synthesized ordered mesoporous Co_3O_4 with a high surface area of 173 m^2/g using three-dimensional(3D) cubic KIT-6 as the hard template, which performed well in the total oxidation of a series of VOCs. To investigate this point, in this work, Co_3O_4 catalysts with different structures(nanoparticles, two-dimensional and three dimensional structures) were prepared and tested for catalytic combustion of methane. The different behaviors of these catalysts for the reaction were compared and the relationship between the performance and catalyst structures was also discussed.

2 Experimental

The details for the materials preparation and characterization as well as the methane catalytic test are available in the Electronic Supplementary Material of this paper.

2D-, 3D-Co_3O_4 catalysts were synthesized using 2D mesoporous SBA-15 and 3D mesoporous KIT-6 as the hard templates, respectively. In a typical synthesis of 3D-Co_3O_4, 10 g of $Co(NO_3)_2\cdot 6H_2O$(99.7%, A. R.) was dissolved in 30 mL of ethanol. Afterwards, 2.0 g of KIT-6 was added. After stirring for 12 h at room temperature, an ultrasonic processing for 1 h was followed to discharge the gas absorbed in the porous channel. The ethanol was removed by evaporation in N_2 atmosphere at 70 °C. The pink powder was further dried in a vacuum drying oven for 6 h at 58 °C. Then the resulting powder was calcined at 200 °C for 2 h followed by calcination at 550 °C for 4 h. The KIT-6 hard templates were removed by NaOH(2 mol/L) solution at 50 °C, followed by centrifugal separation, washing with plenty of deionized water to remove sodium silicate. Then the sample was dried at 100 °C. Finally, the obtained power was 3D-Co_3O_4 catalyst. The 2D-Co_3O_4 catalyst was obtained by the same method which adopting SBA-15 as the template. The nano-Co_3O_4 was prepared by calcining 10 g of $Co(NO_3)_2\cdot 6H_2O$ at 550 °C for 4 h in air, with a heating rate of 1 °C/min.

3 Results and Discussion

The nano-Co_3O_4, 2D-Co_3O_4 and 3D-Co_3O_4 were characterized by N_2 adsorption-desorption, X-ray phototelectron

---

*Corresponding author. E-mail: mengfeiluo@zjnu.cn

Received April 11, 2016; accepted May 19, 2016.

Supported by the National Natural Science Foundation of China(No.21373186).

spectroscopy(XPS) and hydrogen temperature-programmed reduction(H_2-TPR) technique(see the Electronic Supplementary Material of this paper).

The low-angle and wide-angle XRD patterns of Co_3O_4 catalysts are shown in Fig.1. From Fig.1(A), it can be seen that both 2D-Co_3O_4 and 3D-Co_3O_4 catalysts show high diffraction intensity, indicating that they both possess highly ordered mesoporous structure. The 3D-Co_3O_4 catalyst shows three well-resolved diffraction peaks at 1.00°, 1.14° and 1.84°, corresponding to (211), (220) and (332) planes of the channel, respectively. This result indicates that the obtained 3D-Co_3O_4 catalysts has an ordered mesoporous structure with a three-dimensional porous network from its KIT-6 template(*Ia*3*d*)[8]. For the 2D-Co_3O_4, it shows two diffraction peaks at 1.00° and 1.73° corresponding to (100) and (200) planes of the channel, respectively, which indicates that the 2D-Co_3O_4 catalysts also inherits an ordered 2D hexagonal space group structure from its SBA-15 template(*p*6*mm*)[9]. However, the nano-Co_3O_4 catalyst shows no distinct diffraction peak in low-angle XRD, implying the absence of ordered structure in this sample.

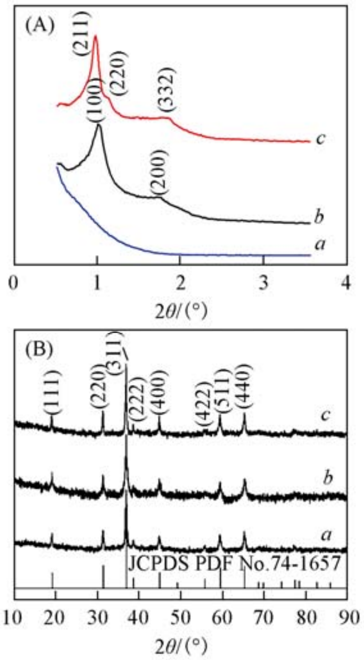

Fig.1 Low-angle(A) and wide-angle(B) XRD patterns of nano-Co_3O_4(*a*), 2D-Co_3O_4(*b*) and 3D-Co_3O_4(*c*) catalysts

The wide-angle XRD patterns of the catalysts[Fig.1(B)] show diffraction peaks at 2*θ* of 19.0°, 31.3°, 36.9°, 38.2°, 44.5°, 55.6° and 65.3°, which are attributed to the cobalt oxide Co_3O_4(JCPDS PDF No.74-1657). These peaks suggest that the cobalt precursor was completely turned into a face centered cubic unit cell of Co_3O_4(space group *Fd*3*m*) with a spinel type structure after calcination[10].

The TEM images of nano-, 2D-, and 3D-Co_3O_4 catalysts are shown in Fig.2. From the low resolution TEM images [Fig.2(A), (D) and (G)] it can be seen that the morphologies of the three Co_3O_4 catalysts are different from each other. The nano-Co_3O_4 shows nano-sized aggregates with irregular shape [Fig.2(A)], the 2D-Co_3O_4 has a group of straight nanorods structure connected by small bridges with a bar shape[Fig.2(D)],

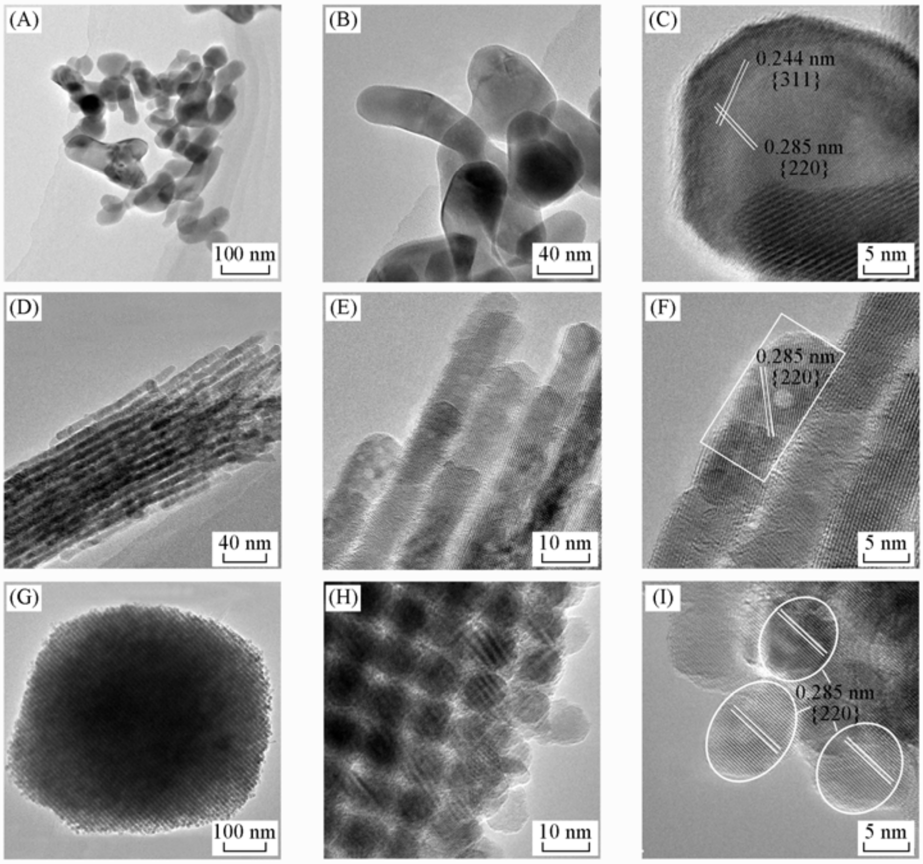

Fig.2 TEM and HRTEM images of nano-Co_3O_4(A—C), 2D-Co_3O_4(D—F), 3D-Co_3O_4(G—I) catalysts

and the 3D-Co_3O_4 possesses a three dimensional bicontinuous channel network with a spherical morphology[Fig.2(G)]. When it goes to higher resolution[Fig.2(B), (E) and (H)], the differences in the structures of 2D-Co_3O_4 and 3D-Co_3O_4 are more obvious. The paralleled nanorods of the 2D-Co_3O_4 has an average diameter of 2—3 nm[Fig.2(E)], while the 3D-Co_3O_4 has an inter-linked network with a mean diameter of about 2—5 nm[Fig.2(H)]. The morphologies of the 2D and 3D-Co_3O_4 catalysts are the perfect replicas of the corresponding silica templates.

The HRTEM images[Fig.2(C), (F) and (I)] further confirm the exposed planes of the catalysts. All the catalysts expose {311}, {220} and {111} planes, with the lattice fringes of 0.244, 0.285 and 0.466 nm, respectively, which is in good consistence with the standard cubic Co_3O_4(JCPDS PDF No.74-1657). Moreover, statistical analyses(one hundred images for each sample, Fig.3) of the catalysts show that the proportions of the exposed {220}, {311} and {111} planes in these catalysts are quite different. In detail, the nano-Co_3O_4 shows 16.7%, 55.6% and 27.7% of {220}, {311} and {111} planes, respectively. The 2D-Co_3O_4 shows 30.6%, 50.0% and 19.4% of {220}, {311} and {111} planes, respectively. The 3D-Co_3O_4 shows 34.8%, 43.5% and 21.7 % of {220}, {311} and {111} planes, respectively. The differences in the percentages of these exposed planes in the catalysts may reflect the confinement effect of the templates(SBA-15 and KIT-6) during the growth of Co_3O_4 crystals[11].

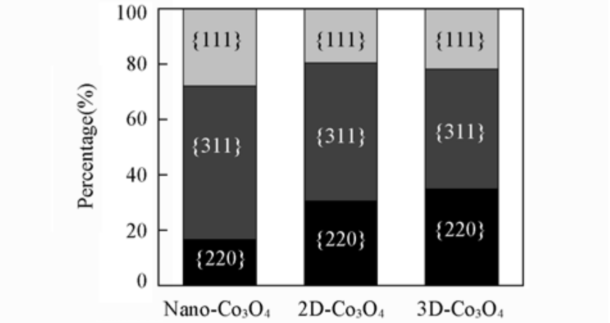

Fig.3 Statistical analyses on the percentages of {220}, {311} and {111} planes that exposed in 100 HRTEM images for different Co_3O_4 catalysts

Fig.4 shows the catalytic oxidation activity of CH_4 over nano-, 2D- and 3D-Co_3O_4 catalysts. It can be clearly seen that the 3D-Co_3O_4 catalyst shows the best catalytic activity with a T_{90} value(the temperature at which a CH_4 conversion of 90% is obtained) of 355 °C, the 2D-Co_3O_4 is less active with a T_{90} of 383 °C, while the nano-Co_3O_4 has the highest T_{90} of 455 °C. Since the surface areas of the catalysts are different, normalized areal specific reaction rates at 300 °C were also calculated and compared(inset of Fig.4). The nano-Co_3O_4 has a reaction rate of 2.09 $nmol\cdot s^{-1}\cdot m^{-2}$; the 2D-$Co_3O_4$ has a reaction rate of 3.27 $nmol\cdot s^{-1}\cdot m^{-2}$ while the 3D-Co_3O_4 has the highest reaction rate(5.88 $nmol\cdot s^{-1}\cdot m^{-2}$). Fig.5 shows the CH_4 catalytic performance with time on stream over nano-, 2D- and 3D-Co_3O_4 catalysts at 400 °C for 12 h, and it can be seen that all the Co_3O_4 catalysts are durable under the reaction condition. Fig.6 shows the TEM images of the fresh 3D-Co_3O_4 catalyst and the used 3D-Co_3O_4 catalyst, and it can be seen that the structure of the 3D-Co_3O_4 catalyst remains intact during the reaction.

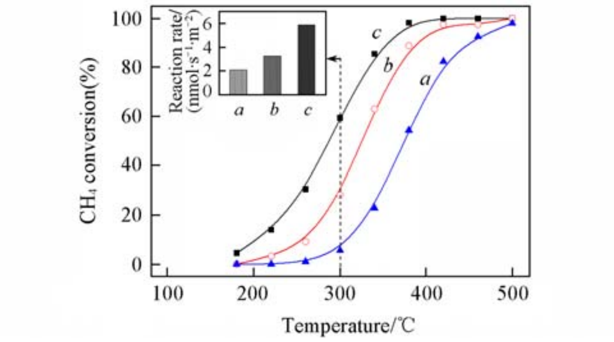

Fig.4 CH_4 conversion as a function of reaction temperature over nano-Co_3O_4(*a*), 2D-Co_3O_4(*b*), 3D-Co_3O_4(*c*) catalysts

The inset shows the CH_4 catalytic activity of different catalysts at 300 °C which is normalized by BET surface area.

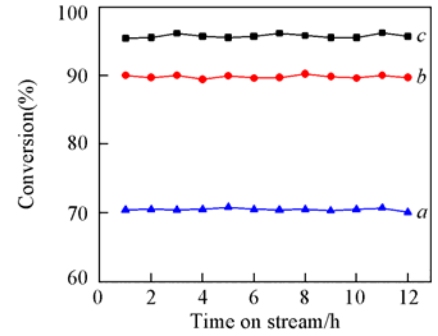

Fig.5 CH_4 catalytic performance with time on stream over nano-Co_3O_4(*a*), 2D-Co_3O_4(*b*), 3D-Co_3O_4(*c*) catalysts

Conditions: temperature: 400 °C; 0.5% CH_4^+, 3% O_2^+, 96.5% N_2, GSHV=12000 $mL\cdot g^{-1}\cdot h^{-1}$.

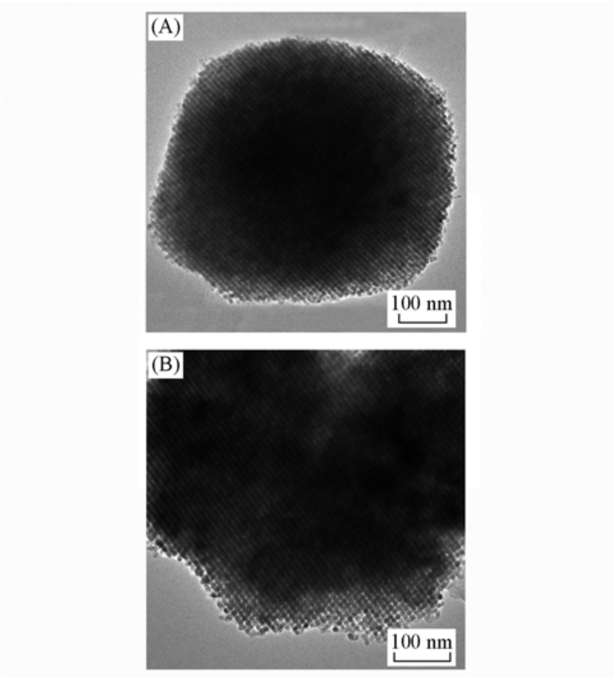

Fig.6 TEM images of fresh 3D-Co_3O_4(A) and used 3D-Co_3O_4(B) catalysts

The comparison of the areal specific reaction rates of the catalysts(inset of Fig.4) strongly implies that the morphologies of the Co_3O_4 are very important for the intrinsic activity, particularly for those with ordered structures(2D-Co_3O_4 and 3D-Co_3O_4). First of all, it has been reported that the ordered mesopores in the Co_3O_4 catalysts are beneficial for the adsorption and diffusion of reactant molecules[12,13]. Such improved adsorption and diffusion of reactants in the 3D-Co_3O_4 therefore could be counted for the enhanced activity. What's more, the structure of Co_3O_4 plays an important role. Since Co_3O_4 has a spinel structure, the Co^{3+} ions in B sites are regarded as the active sites[14]. It has been reported in the literature that the {220} crystal planes in parallel with {110} crystal planes are very active because of the abundance of surface Co^{3+} species, which provide sufficient active sites for the oxidation reaction[15,16]. In the current work, it was found that the 3D-Co_3O_4 has the highest percentage of exposed {220} planes(Fig.3) while the nano-Co_3O_4 has the lowest one. Such preferential exposure of {220} planes is due to the mesopore confinement effect of the template. Therefore, it could be concluded that the exposed {220} plane of Co_3O_4 may significantly contribute to the reactivity.

4 Conclusions

Mesoporous 2D-, 3D-Co_3O_4 catalysts and nano-Co_3O_4 catalysts were tested for the total oxidation of methane. 90% methane conversion over 3D-Co_3O_4, 2D-Co_3O_4 and nano-Co_3O_4 were achieved at 355, 383 and 453 °C, respectively. The methane catalytic activity that normalized by BET surface areas also follows the same order as that of overall catalytic activity. Characterization results showed that the excellent catalytic performance of mesoporous catalysts in methane oxidation can be attributed to their pronounced mesostructure and abundant active Co^{3+} cationic species exposed on the main exposed {220} active crystal planes. The conversion of methane remained the same after the Co_3O_4 catalysts were treated at 300 °C for 12 h. Therefore, the mesoporous Co_3O_4 catalysts especial for 3D-Co_3O_4 catalyst have the best catalysts activity toward methane combustion.

Electronic Supplementary Material

Supplementary material is available in the online version of this article at http://dx.doi.org/10.1007/s40242-016-6141-3.

References

[1] Satsuma A., Tojo T., Okuda K., Yamamoto Y., Arai S., Oyama J., *Catalysis Today*, **2015**, *242*(2), 308

[2] Liotta L. F., Di Carlo G., Longo A., Pantaleoa G., Veneziaa A. M., *Catalysis Today*, **2008**, *139*(3), 174

[3] Lapisardi G., Urfels L., Gélin P., Primeta M., Kaddouria A., Garbowskia E., Toppib S., Tenab E., *Catalysis Today*, **2006**, *117*(4), 564

[4] Persson K., Jansson K., Järås S. G., *Journal of Catalysis*, **2007**, *245*(2), 401

[5] Hu L., Peng Q., Li Y., *J. Am. Chem. Soc.*, **2008**, *130*(48), 16136

[6] Sutthiumporn K., Kawi S., *International Journal of Hydrogen Energy*, **2011**, *36*(22), 14435

[7] Garcia T., Agouram S., Sánchez-Royo J. F., Murillo R., Mastral A. M., Aranda A., Vázqueze I., Dejoze A., Solsona B., *Applied Catalysis A: General*, **2010**, *386*(1), 16

[8] Kleitz F., Bérubé F., Guillet-Nicolas R., Yang C. M., Thommes M., *J. Phys. Chem. C*, **2010**, *114*(20), 9344

[9] Zhao D., Huo Q., Feng J., Chmelka B. F., Stucky G. D., *J. Am. Chem. Soc.*, **1998**, *120*(24), 6024

[10] Wang Y., Yang C. M., Schmidt W., Spliethoff B., Bill E., Schüth F., *Adv. Mater.*, **2005**, *17*(1), 53

[11] Tüysüz H., Lehmann C. W., Bongard H., Tesche B., Schmidt R., Schüth F., *J. Am. Chem. Soc.*, **2008**, *130*(34), 11510

[12] Xia Y., Dai H., Jiang H., Zhang L., *Catal. Commun.*, **2010**, *11*(15), 1171

[13] Tüysüz H., Comotti M., Schüth F., *Chem. Commun.*, **2008**, (34), 4022

[14] Xie X., Shen W., *Nanoscale*, **2009**, *1*(1), 50

[15] Bai B., Arandiyan H., Li J., *Applied Catalysis B: Environmental*, **2013**, *142*(1), 677

[16] Xie X., Li Y., Liu Z. Q., Haruta M., Shen W., *Nature*, **2009**, *458*(7239), 746